

Investigation of the superconducting energy gap in the compound $\text{LuNi}_2\text{B}_2\text{C}$ by the method of point contact spectroscopy: two-gap approximation

N. L. Bobrov, S. I. Beloborod'ko, L. V. Tyutrina, V. N. Chernobay, I. K. Yanson *
*B.I. Verkin Institute for Low Temperature Physics and Engineering,
 NAS of Ukraine, 47, Lenin Prospect, 61103, Kharkiv, Ukraine*

D. G. Naugle and K. D. D. Rathnayaka
Department of Physics Texas A&M University, College Station TX 77843-4242, USA
 (Dated: July 4, 2018)

It is shown that the two-gap approximation is applicable for describing the $dV/dI(V)$ spectra of $\text{LuNi}_2\text{B}_2\text{C}$ -Ag point contacts in a wide interval of temperatures. The values and the temperature dependences of the large and the small gaps in the ab plane and in the c direction were estimated using the generalized BTK model²⁰ and the equations of.²¹ In the BCS extrapolation the critical temperature of the small gap is 10 K in the ab plane and 14.5 K in the c direction. The absolute values of the gaps are $\Delta_0^{ab} = 2.16 \text{ meV}$ and $\Delta_0^c = 1.94 \text{ meV}$. For the large gaps the critical temperature coincides with the bulk T_c , $T_c^{bulk} = 16.8 \text{ K}$, and their absolute values are very close, being about 3 meV in both orientations. In the c direction the contributions to the conductivity from the small and the large gaps remain practically identical up to $10 \div 11 \text{ K}$. In the ab plane the contribution from the small gap is much smaller and decreases rapidly as a temperature rises.

PACS numbers: 63.20.Kr, 72.10.Di, 73.40.Jn

I. INTRODUCTION

Compounds $\text{ReNi}_2\text{B}_2\text{C}$ (Re is a rare earth metal) have a tetrahedral crystal structure (e.g., see¹ Fig. 6) with the spatial group $I4/mmm$ ¹ and the characteristic parameters: two lattice constants a and c ($a = 3.46 \text{ \AA}$, $c = 10.63 \text{ \AA}$ for $\text{LuNi}_2\text{B}_2\text{C}$) and the distance z between the B atom and the RC plane. The anisotropy in these compounds is determined by the ratio c/a and is rather high ($c/a \sim 3$).¹

According to electron structure calculation, $\text{ReNi}_2\text{B}_2\text{C}$ compounds are three-dimensional metals in which all atoms contribute to the density of states at the Fermi surface.^{2,3,4} In $\text{LuNi}_2\text{B}_2\text{C}$ three energy bands crossing the Fermi level subdivide the Fermi surface into three distinct regions: (1) two spheroidal sheets at Γ -points that are extend along the c axis; (2) two flat P-centered square regions with the sides parallel to $\langle 100 \rangle$ and $\langle 010 \rangle$, and finally (3) the largest basic X-centered part mostly cylindrical in shape (closely resembling practically two-dimensional crystal structure) whose axis is parallel to the c axis.^{2,3,4} In this sheet there are flat regions at the points $0.56 \pm (2\pi/a)$, the nesting, typical for the compounds of this family.⁴ It is precisely these features that determine the Kohn anomaly near the wave vector $Q_m \approx (0.5, 0, 0)$ ^{5,6} and the incommensurate ordering with $Q_m \approx (0.5, 0, 0)$ in AFM compounds. The part of the Fermi surface responsible for nesting makes only $(4.4 \pm 0.5\%)$ and shows up a slightly increased resistance for the current along $\langle 100 \rangle$.⁴

As was shown for point contacts with a ballistic transit of electrons in a many-band superconductor⁷, in any di-

rection the contribution to conductivity from each band is proportional to the area of the Fermi surface projection from the corresponding band onto the interface. Since the fraction of the Fermi surface responsible for nesting is small, the nesting-related features are not obvious in the point-contact spectra.

Thus, the Fermi surface of nickel borocarbides consists of several bands: it is anisotropic and corresponding Fermi velocity v_F varies within wide limits. In this case T_c is determined not by the total density of states $N(E_F)$, but by the narrow peak of the density of states at the Fermi level (see¹, Fig. 12). The density-of-states peak is induced by the slow electrons from the flat (nesting) regions of the Fermi surface with the wave vectors $(0.5-0.6, 0, 0)$.¹

In the normal state the resistivity ρ is isotropic because it is connected with the groups of electrons that have rather high velocities v_F and do not belong to the flat regions of the Fermi surface.¹ The temperature dependence of resistance ρ in single crystal $\text{YNi}_2\text{B}_2\text{C}$ and $\text{LuNi}_2\text{B}_2\text{C}$ also exhibits this practically isotropic metallic behavior (see¹, Fig. 11).

The scanning tunnel microscope measurements on $\text{LuNi}_2\text{B}_2\text{C}$ give a rather low value of superconducting energy gap along the c axis (4.2 K), $\sim 2.2 \text{ meV}$ ($2\Delta/kT_c = 3.2$).^{8,9} In the ab plane ($T \sim 0.3 \div 0.5 \text{ K}$) for $\text{YNi}_2\text{B}_2\text{C}$ the gap data are greatly scattered, from 2.3 meV ¹⁰ to 3.5 meV ¹¹ ($2\Delta/kT_c = 3.44 \div 5.24$). The high ratio in¹¹ can be attributed to the estimation procedure: the gap was estimated from the positions of the maxima in the differential conductivity curve. The shape of the curve, however, suggests a considerable variation of the gap over the Fermi surface, and the cited value of the gap is closer to its maximum rather than to its average magnitude. For a number of nickel borocarbides the ratio obtained

*Email address: yanson@ilt.kharkov.ua

from point contact measurements in the ab plane^{12,13} is $2\Delta/kT_c = 3.7 \div 3.8$.

In the recently discovered superconductor MgB_2 the Fermi surface is formed by two groups of energy bands having different dimensions, which determines a two-gap conductivity¹⁴. Similarly, we can expect a many-gap conductivity in nickel borocarbide compounds. Note that the dHvA data^{15,16} also point to the presence of at least two or even three groups of the Fermi velocities evidencing in favor of a two or three-band model. In¹⁷ the behavior of $H_{C2}(T)$ is considered within a two-band model. One band has low Fermi velocities, high $H_{C2}(0)$, T_c , λ (electron-phonon interaction) parameters. However, all these characteristics are suppressed in the bound system by another band with high Fermi velocities and smaller superconducting parameters. In this case the two-gap approximation commonly used for two-band superconductors¹⁸ seems quite reasonable.

Here we report the results on energy gap anisotropy that were obtained on the nickel borocarbide superconductor $\text{LuNi}_2\text{B}_2\text{C}$ for the main crystallographic orientations - in the ab plane and along c axis. This study is a logical extension of¹⁹. It was shown that the one-gap approximation could not provide an accurate description of the experimental curves in the low temperatures region and use of the two-gap approach was contemplated.¹⁹ The largest and the smallest gaps were estimated in the ab plane and along c direction at $T \ll T_c$. Besides, using the generalized BTK²⁰ and Beloborodko's²¹ models, the lowest values of the largest gap were estimated in these directions as a function of temperature.¹⁹ Owing to the high quality of the experimental curves (no "humps", or broad maxima at $|eV| > \Delta$), the estimation was possible in the "wings", i.e. in the regions of the experimental curves where the biases are higher than that at the differential resistance minima ($|eV| \approx \Delta$).

Below we show the results of the two-band calculation for $\text{LuNi}_2\text{B}_2\text{C}$ obtained within two models^{20,21} for experimental curves obtained before.¹⁹ In our opinion, the calculation most closely corresponds to the many-band character of the Fermi surface in these compounds. The anisotropy is estimated qualitatively in each band using the parameter Γ in the BTK model,²⁰ or γ in Beloborodko's model.²¹ The calculation is compared with the results of one-gap fitting.¹⁹

II. EXPERIMENTAL TECHNIQUE

The point-contact measurement was performed on single crystal $\text{LuNi}_2\text{B}_2\text{C}$ ($T_c \simeq 16.9\text{ K}$) grown by Canfield and Budko using a flux method.²² The crystals were thin ($0.1 \sim 0.2\text{ mm}$) plates with the c axis perpendicular to the plane of the plate. The single crystal surface always has quite a thick layer on it in which superconductivity is either absent or strongly suppressed. Point contacts between natural crystal faces therefore suffer from this disadvantage. For measurement in the ab plane, the

crystal is usually cleaved, and the point contact is made between a metallic counterelectrode and the cleaved surface. The cleavage perpendicular to the c direction is a technical challenge. To do this, the crystal surface was cleaned with a $10 \div 15\%$ HNO_3 solution in ethanol for several minutes. The properly etched crystal has metallic luster and its surface is free from colored film. The crystal was washed thoroughly in pure ethanol and then installed in contact-making device. As found subsequently, the etching conditions are very important for producing high-quality point-contacts.²³ In the ab plane the measurements results seem to be indifferent to cleavage or etching - they are practically similar in both cases. But a deeper analysis (see below) reveals certain distinctions caused by defects in the cleavage surface. The other electrode was made of high-purity silver. The point contacts in the ab plane were fabricated between the edge of the prism-shaped Ag electrode and freshly cleaved (etched) face of the single crystal (shear technique²⁴). The deviation from the direction perpendicular to the c axis varied within $5 \div 10^\circ$. To make a contact in the c direction, the "needle-anvil" geometry was used. The needle radius was 1-3 microns. The temperature was measured with a special insert (similar to that in²⁵).

The point contact resistance varied typically from several Ohms to tens of Ohms. To attain more detailed data, we selected point-contacts with the greatest possible tunneling which was judged from the presence of a differential resistance maximum at zero bias and the highest non-linearity of the I - V curves at biases $\pm\Delta$ typical for a non-perturbed superconducting surface in the contact neighborhood. Unfortunately, we were able to take a complete set of curves in the whole range $T_{\min} \approx 1.5\text{ K} \rightarrow T_c$ only on a few contacts. Because of high resistance and long-term (over 10-12 hours) measurements of temperature, many of contacts were broken down. The measurements were made with the nearly equal temperature steps. There were taken 47 curves in the c direction and 41 curves in the ab plane.

III. DATA PROCESSING

Some curves of the temperature series for the first derivatives dV/dI of the $\text{LuNi}_2\text{B}_2\text{C}$ - Ag point contacts in the c direction and in the ab plane are shown in Fig. 1. The contact diameters were calculated by Sharvin's equation using $R_0^{ab} = 22.5\Omega$, $R_0^c = 45\Omega$, $\rho l = 11.25 \cdot 10^{-16}\Omega\text{m}^2$ of¹⁷ and allowing for the presence of a potential barrier in the constriction region: $Z_{ab} = 0.7$, $Z_c = 0.55$. The obtained diameters $d_{ab} = 13.7\text{ nm}$ and $d_c = 8.5\text{ nm}$ are very close in the order of magnitude to the coherence length in this compound ($\xi = 6.5\text{ nm}$ ¹⁷). The measured curves were symmetrized $dV/dI_{Sym} = 1/2[dV/dI(V) + dV/dI(-V)]$ and normalized to the normal state at $T > T_c$.

Two approaches were used to compare the theoretical and experimental results obtained in the one- and two-

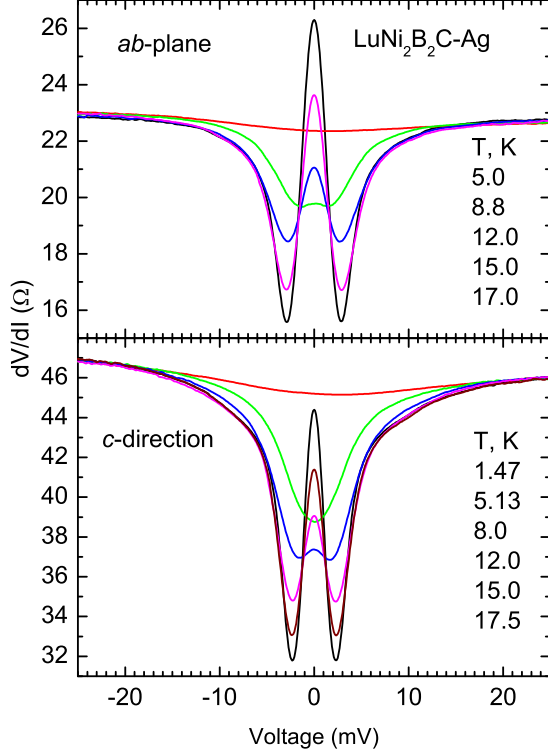


FIG. 1: Differential resistances of $\text{LuNi}_2\text{B}_2\text{C-Ag}$ point contact at different temperatures. To avoid crowding, only several curves are shown.

gap approximation. First, a model was applied, which describes the electrical conductivity of pure $S - c - N$ point contacts in the presence of an arbitrarily transparent potential barrier at the boundary between the metals. The model allows for the finite lifetime of Cooper pairs.²¹ The equations describing the $I - V$ characteristics of the point contact within this model are given in.^{19,21} The model, however, interprets the superconducting order parameter and the energy gap as distinct magnitudes. The BCS order parameter Δ was found from

$$\Delta = \lambda \int_0^{\omega_D} d\varepsilon \tanh\left(\frac{\varepsilon}{2T}\right) \text{Re} \frac{1}{\sqrt{u^2 - 1}} \quad (1)$$

where u is obtainable by solving the equation

$$\frac{\varepsilon}{\Delta} = u \left[1 - \frac{\gamma}{\sqrt{1 - u^2}} \right] \quad (2)$$

The energy gap Δ_0 and the order parameter Δ are related as

$$\Delta_0 = \Delta \left(1 - \gamma^{2/3} \right)^{3/2} \quad (3)$$

Here $\gamma = 1/(\tau_s \Delta)$ is the pair breaking parameter, τ_s is the mean free time during spin-flip scattering at impurities. When magnetic impurities are absent, τ_s tends to infinity and the equations describing the $I - V$ characteristics in²¹ and in²⁶ coincide.

The other approach was based on the generalized Blonder-Tinkham-Klapwijk (BTK) model commonly used to describe $S - c - N$ point contacts. The model allows for finite lifetime of quasiparticles $\tau = \hbar/\Gamma$ determined by inelastic scattering, which leads to the broadening of the density of states in the superconductor²⁰. Formally, according to the previous theory, the BTK-based results are obtained under condition of strong pair breaking ($|u| \gg 1$)²¹. Therefore, in the strict sense, the generalized BTK model contains no gap. For any infinitesimal broadening parameter Γ , at $T = 0$ the density of states near Fermi surface is nonzero. In theory²¹, the order parameter is qualitatively analogous to the pseudogap in the generalized BTK model.

In the two-gap approximation, the general conductivity of the point contact is taken as a superposition of the conductivities from two regions of the Fermi surface having their own gaps. In this case the experimental curves were fitted using the expression

$$\frac{dV}{dI} = \frac{S}{\frac{dI}{dV}(\Delta_1, \gamma_1, Z)K + \frac{dI}{dV}(\Delta_2, \gamma_2, Z)(1-K)} \quad (4)$$

K is the coefficient, characterizing the contribution from the part of the Fermi surface with the gap Δ_1 , S is the scaling factor describing the intensity of the experimental curve. It is used to make the amplitudes of the theoretical and experimental curves equal. The best agreement between the shapes of the theoretical and experimental curves corresponding to the minimum *rms* deviation in the curve $F(\Delta)$ was taken as the main criterion of fitting in both the models at low and moderate temperatures. When the temperature increases, the curves $F(\Delta)$ become flatter, which entails much uncertainty in estimation of Δ . In this case the scale-factor S is of primary importance. It is, as a rule, independent of temperature and at low temperatures it can be calculated quite accurately through averaging. The details of the calculation in the one-gap and two-gap approximations are offered in the Appendix.

IV. CALCULATION

A. One-gap approximation

Although $\text{LuNi}_2\text{B}_2\text{C}$ exhibits a two-band kind of superconductivity, its experimental curves can be described in the zero approximation with an averaged gap possessing the broadening parameter Γ or the pair-breaking parameter γ . The temperature dependences of the order parameters (the model of²¹) and the gaps (BTK calculation²⁰)

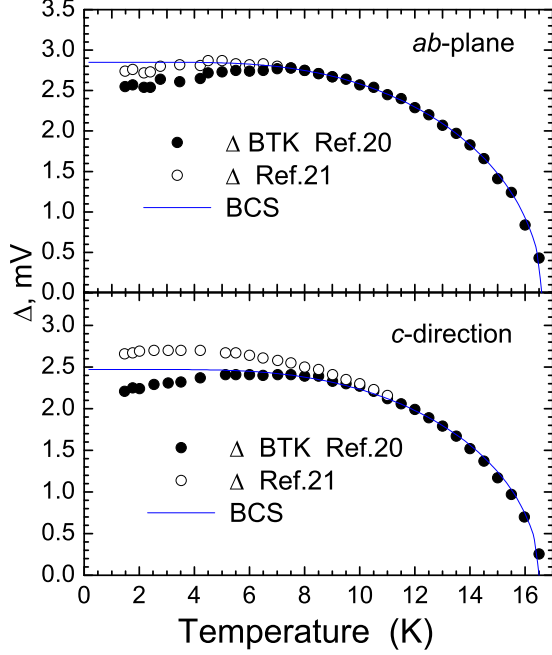


FIG. 2: Temperature dependences of the order parameter (energy gap) Δ calculated in the one-gap approximation²¹ (open circles) and within the generalized BTK model²⁰ (solid circles) for point contact LuNi₂B₂C-Ag in the *ab* plane and in the *c* direction. Solid lines show the BCS approximation. Here and in all other figures the following symbols are used: circles - one-gap or average gap calculation; squares - the small gap; triangles - the large gap; closed symbols - BTK calculation Ref. 20; open symbols - calculation by formulae of Ref. 21

in the *ab* plane and in the *c* direction are shown in Fig. 2 along with the BCS curves.

In both cases we observe a deviation from the BCS curve. In the *c* direction the deviation is towards higher values when the calculation is based on²¹ and towards lower values in the BTK approximation. As for the *ab* plane, it should be noted that in the low temperature region the resistance of the contact varied during the measurement and became stable only at 4 K. This may be the reason why in both models the deviations from the BCS dependence in the low temperature region descend to lower values. The results of the both approximations start to coincide near 8 K in the *ab* plane and near 11 K in the *c* direction. Precisely at these temperatures (see Fig. 3), the parameters γ (pair breaking) or Γ (broadening) turn to zero in these orientations.

The ratio Γ/Δ or the γ magnitude can be used for semiquantitative estimation of the contribution of the two-band structure to the point contact conductivity. Since in the *c* direction the ratio Γ/Δ is $1.5 \div 2$ times higher, we can expect a stronger two-band effect in it.

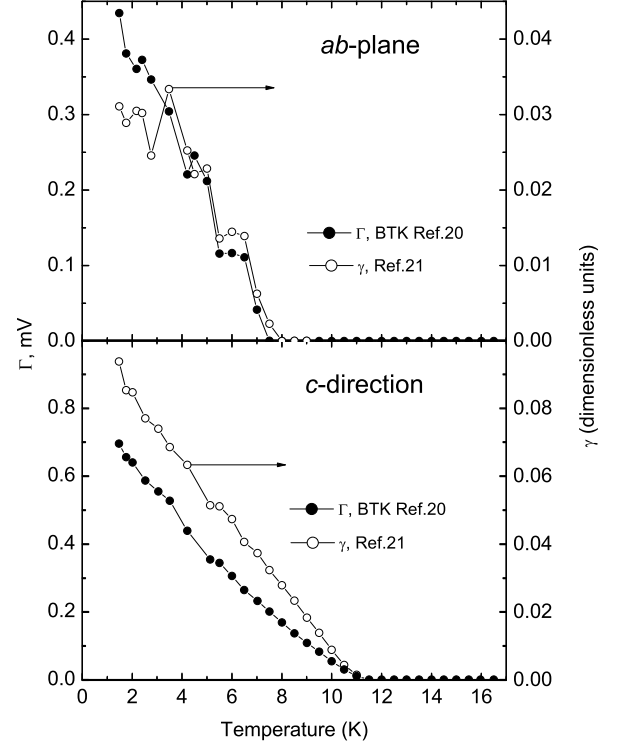


FIG. 3: Temperature dependences of broadening Γ (closed circles) and pair-breaking γ (open circles) parameters for LuNi₂B₂C-Ag point contact in the *ab* plane and in the *c* direction in the one-gap approximation.

Besides, we can conclude that the experimental curves demonstrate one-gap superconductivity above 8 K in the *ab* plane and above 12 K in the *c* direction. True, the more accurate two-band calculation (see below) gives somewhat different results; nevertheless, this technique is quite good for semiquantitative calculation. Note that in the strict sense, neither Γ nor γ are meant for describing distribution of gaps over the Fermi surface. They allow for the finite lifetime of carriers, which only simulates the energy gap anisotropy. Their use in this particular case is, however, quite justified as it enables an approximate modeling of the $I - V$ characteristic in the $N - c - S$ point contact.

In *ab* and *c* orientations the gap is anisotropic, though observed anisotropy is rather low (see Figs. 1,2). Statistically (several tens of contacts were examined for each direction), the positions of the dV/dI -minima characterizing the gap value are $15 \div 20\%$ shifted towards higher energies in the *ab* plane.

In addition to the deviation from the BCS $\Delta(T)$ -curve, the one-gap model also fails to provide a good fitting of the shapes of theoretical and experimental $dV/dI(V)$ -curves. The one-gap fitting (BTK model²⁰) of experi-

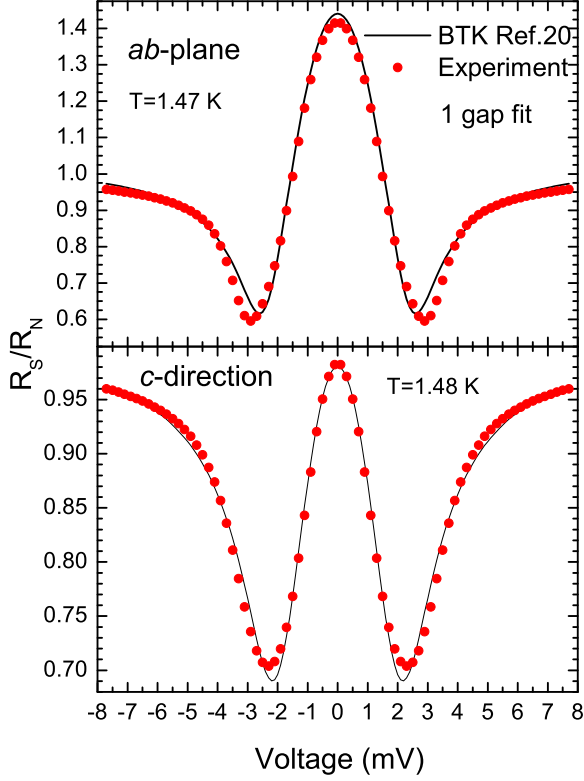


FIG. 4: Fitting of experimental curves in the one-gap approximation (BTK model²⁰) for LuNi₂B₂C-Ag point contact. A few experimental points are shown to avoid overloading.

mental curves is shown in Figs. 4 and 5 illustrates the temperature dependences of the *rms* deviations between the shapes of the theoretical and experimental curves. The best agreement is observed above $7 \div 8$ K.

We attribute this rather high value to the two-band character of the superconductivity. This indicates that experimental curves must be fitted in the two-gap approximation, as in the case of MgB₂ and¹⁹.

B. Two-gap approximation

The two-gap fitting of experimental curves in the low temperature region is illustrated in Fig. 66. The agreement is seen to be much better than with the one-gap approximation (compare with Fig. 4).

The temperature dependences of the order parameters calculated from²¹ (open symbols) and the gaps calculated within the generalized BTK model²⁰ (solid symbols) in the *ab* plane and along the *c* axis are shown in Fig. 7 along with the corresponding BCS dependences (solid lines). In addition to the small Δ_1 (squares) and large Δ_2 (triangles) gaps, Fig. 7 illustrates for a comparison an averaged gap Δ_M (circles) which allows for the partial

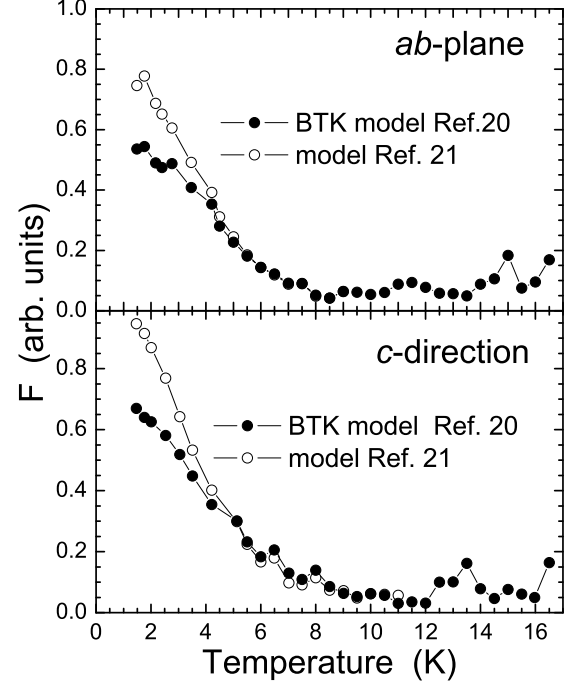


FIG. 5: Temperature dependences of the *rms* deviation characterizing shape discrepancies between experimental and theoretical (calculation by Ref. 21 curves (open circles) and in the BTK model Ref. 20 (closed circles)) for LuNi₂B₂C-Ag point contact in the *ab* plane (a) and *c* direction (b) in the one-gap approximation.

contributions to the conductivity of the contact made by the Fermi surface areas with different gaps (see formula in Fig. 7).

It is interesting to compare the BCS approximation of the critical temperatures of the small gap in the *ab* plane and in the *c* direction: $T_c^{ab}(\Delta_1) = 10$ K and $T_c^c(\Delta_2) = 14.6$ K. The absolute values of the small gaps are close ($\Delta_0^{ab} = 2.16$ mV, $\Delta_0^c = 1.94$ mV), the difference being no more than 10%. The critical temperatures of the large gaps are similar and coincide with the bulk $T_c = 16.8$ K. The values of the large gaps are about $\Delta_2 = 3$ mV. Note that both the models give practically identical results for the large and the small gaps (open and closed triangles and squares). As for the average gaps (circles), their values in the low temperature region are dependent on the model applied. This is because of different correlations between the partial contributions from the large and the small gaps (see Fig. 8).

It thus turns out that the higher Γ (or γ) in the *c* direction (where the two-band character is more pronounced) obtained in one-gap approximation is determined not by the difference between the values of the large and the small gaps but by the difference between the partial con-

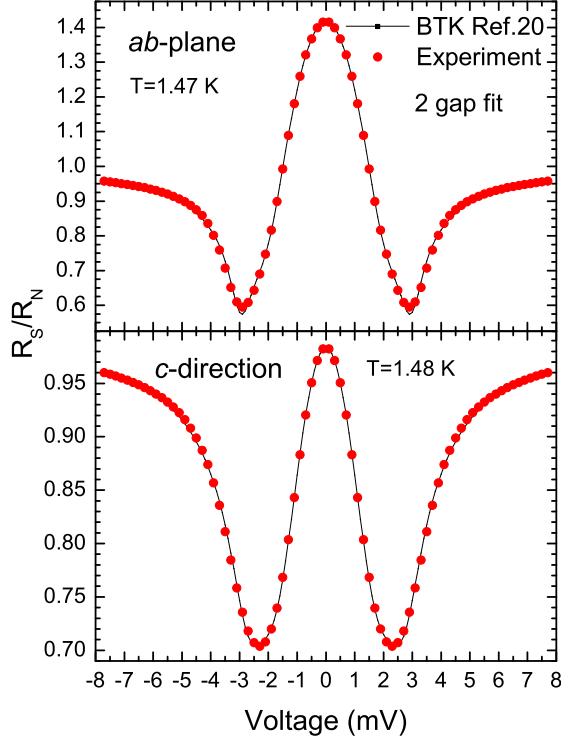


FIG. 6: Two-gap approximation (BTK model Ref. 20) of experimental curves for LuNi₂B₂C-Ag point contacts. To avoid crowding, only a part of experimental points is shown.

tributions from these gaps. In the *ab* plane the contribution of the small gap (open squares, Fig. 8 upper panel) is smaller than in the *c* direction and it decreases rapidly as the temperature rises. In the *c* direction the contributions from both gaps are very close (in average between the two models^{20,21} is about 50% for each) up to 10 ÷ 11 K. (Note that in the BTK calculation²⁰ the contribution from Δ_1 is over 50%; in the calculation by model of²¹ the Δ_1 contribution is below 50% and in average the contribution from Δ_1 is close to that from Δ_2 at low temperatures.)

The temperature dependence of γ (pair breaking), or Γ (broadening of quasiparticle levels) obtained in the two-gap approximation are shown in Fig. 9.

Note that the parameters Γ and γ are considerably higher for the small gap both in the *ab* plane and in the *c* direction. Their ratios to the corresponding gaps are larger too: $(\Gamma_1/\Delta_1) = 0.185 > (\Gamma_2/\Delta_2) = 0.021$ in the *ab* plane and $(\Gamma_1/\Delta_1) = 0.333 > (\Gamma_2/\Delta_2) = 0.1$ in the *c* direction. As stated above, we consider that these ratios simulate qualitatively to what extent the gap is distributed over the corresponding sheet of the Fermi surface. We can thus assume that at low temperatures the value of the gap changes very little for the part of the

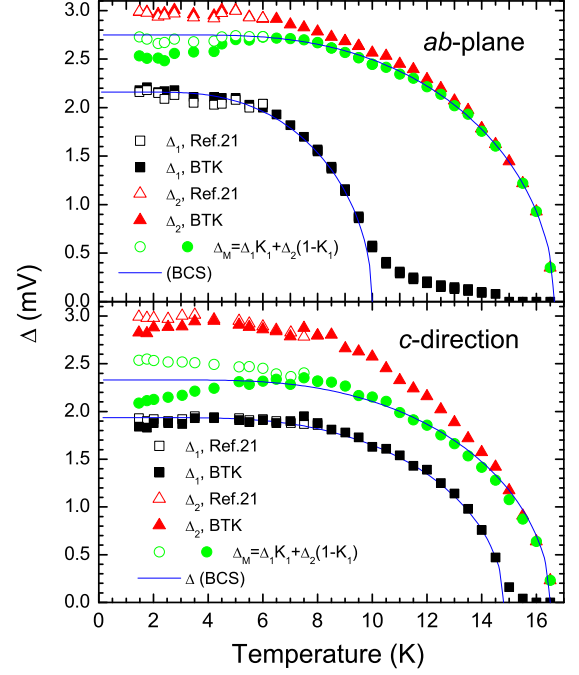


FIG. 7: Temperature dependences of the order parameter (energy gap) Δ calculated in the two-gap approximation using the equation of Ref. 21 (open circles) and the BTK model Ref. 20 (solid circles) for LuNi₂B₂C-Ag point contacts in the *ab* plane (a) and *c* direction (b). Solid lines - BCS extrapolation. In addition to the large Δ_2 (triangles) and small Δ_1 (squares) gaps, the figure includes medium gaps Δ_M (circles) that were obtained taking into account the partial contribution to the contact conductivity from the Fermi surface regions with the large and small gaps (see the formula in the figure and Eq.(4) in the text).

Fermi surface with the larger gap (Δ_2). In the small-gap region (Δ_1), the gap is spread over a considerably broader range of energies at low temperatures. Thus the two-gap approximation, even being more accurate, cannot describe the experimental curves in the whole T -interval. This is evident (see Fig. 10) in the temperature dependences of the *rms* deviations F between the shapes of the fitted and experimental curves (even for two-gap calculation).

Although the errors observed (the F magnitude) are much lower (about half as high at the lowest temperature) than in the one-gap case (Fig. 5), they increase appreciably below $T = 4.5 \div 5$ K. This may occur because the three-band conductivity comes into play, which must not be ruled out completely for this compound. Proceeding from the significantly higher ratio Γ_1/Δ_1 at low temperatures, we can treat the small gap in its turn as a superposition of two different gaps with different T_c . These gaps are close to each other and their energies

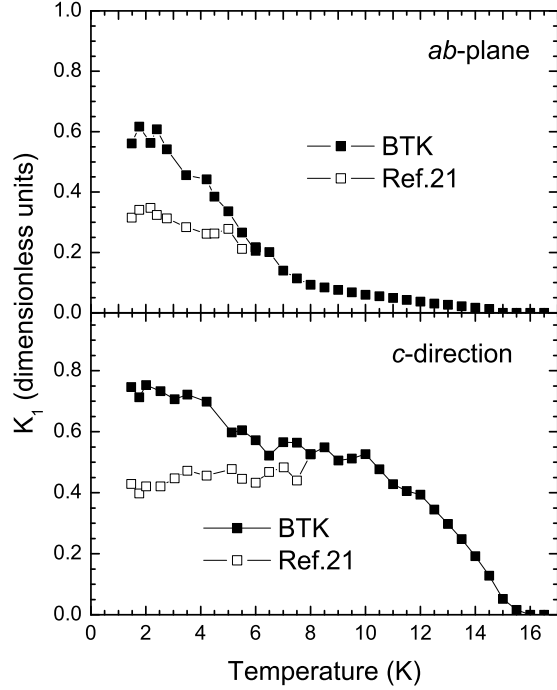


FIG. 8: Temperature dependences of the partial contribution to the contact conductivity from the small gap (calculation by the formula of Ref. 21 and within the BTK model Ref. 20. Also, see Eq.4 in the text.

overlap. The temperature dependence of the error (F) suggests that we can expect $T_c \approx 5$ K for the smallest gap in the BCS approximation. This is the lowest estimate. However, because Γ_2 becomes zero at 6 K (a plane) and 8 K (c direction) (Fig. 9), it is possible that precisely these temperatures are closest to T_c of the gap in the third band.

V. DISCUSSION

In our experiments we have not succeeded in detecting noticeable anisotropy of the energy gap in the ab plane and in the c direction. It was no more than 20% in the average-gap approximation. The reason may be a rough cleavage surface, which made it difficult to fix the contact axis precisely along a direction where the gap minimum is predicted. Therefore, following the common practice in point contact spectroscopy, we tried to select point contacts with the highest superconducting parameters (gaps, $I - V$ nonlinearities). Since in the ab plane the maximum gap is predicted in the $\langle 110 \rangle$ direction, our contacts probably were made to correspond most closely to this orientation. Besides, the angular selectivity of point contact measurement is not high enough. Since tunneling

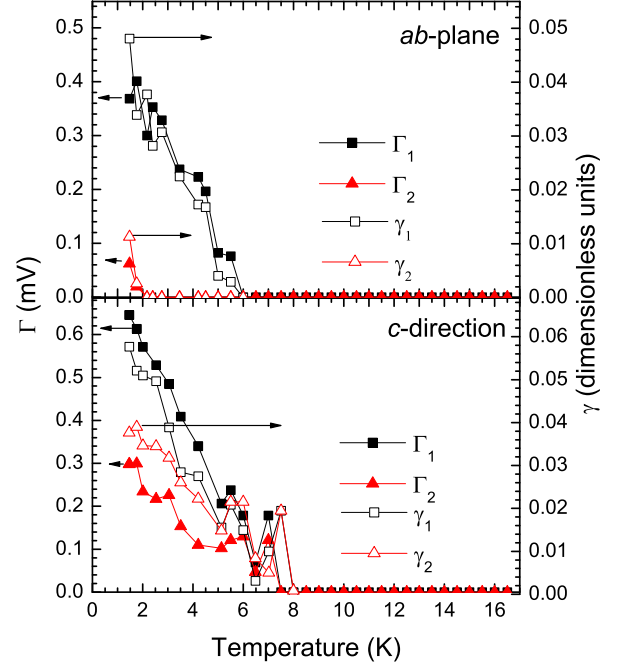


FIG. 9: Temperature dependences of the broadening Γ (closed circles) and pair-breaking γ (open circles) parameters for LuNi₂B₂C-Ag point contact in the ab plane (a) and in the c direction (b) in the two-gap approximation. Note that the parameters are considerably higher for the small gaps (squares).

component in the point contacts is rather weak (the Z coefficient is not high) and their diameters are close to the coherence length, it is quite likely that the conversion of the electrons into pairs in the vicinity of the contact occurs within a spherical geometry. According to Maki's model²⁷ the angle between the largest and the smallest gaps in the ab plane is 45° . As a result, the spectra taken in these directions can hardly have big distinctions. The most obvious features discovered by us are the different critical temperatures of the small gap in the ab plane and in the c direction obtained in the BCS extrapolation (Fig. 7).

With the evidence available, it is hardly possible to conclude unambiguously whether this phenomenon is related to the gap anisotropy or any other (e.g., technological) factor. In the ab plane the point contact was formed on a freshly cleaved surface. In the c direction the surface was cleaned chemically and experienced no mechanical stress. It is known that elastic scatterers first cause gap isotropization, then reduce the gap and suppress the critical temperature. Although in our experiments the critical temperatures of the point contacts coincide with T_c of the bulk, the partial T_c of the small gap (~ 10 K Fig.

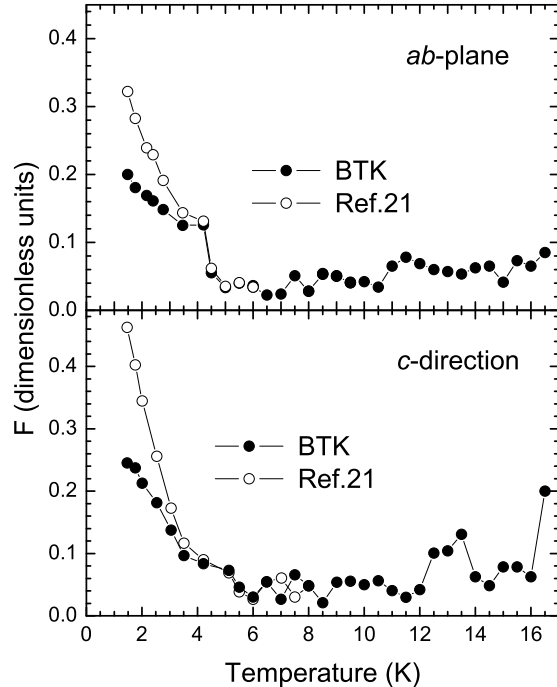


FIG. 10: Temperature dependences of the *rms* deviation characterizing shape discrepancies between experimental and theoretical curves (calculation by the equations of Ref. 21 (open circles) and in the BTK model Ref. 20 (solid circles)) for $\text{LuNi}_2\text{B}_2\text{C}$ -Ag point contacts in the *ab* plane (a) and in the *c* direction (b) in the two-gap approximation.

7) and its relative contribution (coefficient K_1 Fig. 8) to the general conductivity decreases in the *ab* plane, which indicates isotropization of the general gap in this plane. To clear up possible reasons for this phenomenon, further measurements on chemically cleaned natural growth faces of single crystals in the *a* direction are needed.

According to Pokrovsky's theorem^{28,29} in the case of anisotropic one-gap superconductivity, the temperature dependence of the gap is independent of crystallographic directions. In our case the temperature dependences of the large and the small gaps and the BCS extrapolation of the critical temperatures are quite different. This prompts the conclusion that this behavior can not be caused by the contributions to conductivity made by a single anisotropic superconducting gap in different crystallographic directions. On the contrary, we observe the indications of two different superconducting gaps from different energy bands.

Noteworthy also is another point, namely, the limits of applicability of the two-gap approach to describing experimental data. In the strict sense, the method requires that the broadening (pair breaking) parameters should be zero for both gaps. This condition is met at $T > 6$ K

for *ab* plane and $T > 8$ K in the *c* direction (see Fig. 9). At lower temperatures the gaps do not have strictly specified values as they are distributed over a certain range of energies simulated by nonzero Γ or γ . In the *ab* plane the largest gap stands out as an individual line above 2 K, while in the *c* direction both the gaps start broadening at nearly the same temperature. As the temperature lowers, the distribution extends up to overlapping of energies. This brings more uncertainty into the description of curves in the two-band approximation (Fig. 10) and sends us in search of a new method. A possible technique of a more adequate description of our experimental results near $T = 1.5$ K is illustrated in¹ (Figs. 12-14).

VI. CONCLUSIONS

This study demonstrates that the two-gap approximation is more appropriate for describing the superconductivity of $\text{LuNi}_2\text{B}_2\text{C}$ in a wide interval of temperatures. The values and the temperature dependences of the large and the small gaps have been estimated for *ab* plane and the *c* direction. It is found that in the BCS extrapolation of the critical temperature for the small gap is $T_c = 10$ K in the *ab* plane and $T_c = 14.5$ K in the *c* direction. The absolute values of the gaps are $\Delta_0^{ab} = 2.16$ meV, $\Delta_0^c = 1.94$ meV. For the large gaps T_c coincides with T_c^{bulk} : $T_c(\Delta_2) = 16.8$ K and their absolute values are very close in both orientations, being about 3 meV. It is found that in the *c* direction the contributions to conductivity from the small and the large gaps are nearly equal up to 10 ÷ 11 K. In the *ab* plane the contribution of the small gap is considerably weaker and decreases rapidly as the temperature is growing.

Acknowledgment

The single crystal samples for this study were graciously provided by P.C. Canfield and S.L. Budko at Ames Laboratory and Iowa State University. The authors are indebted to Yu.G. Naidyuk for helpful discussions. The work was supported in terms of the complex program of fundamental research "Nanosystems, nanomaterials and nanotechnologies" of the National Academy of Sciences of Ukraine (*Project No* 10/05-N). The work was supported in part by the Robert A. Welch Foundation (*Grant No* A - 0514, Houston, TX), The Telecommunications and Informatics Task Force at Texas A&M University, the Texas Center for Superconductivity at the University of Houston (*TCSUH*) and the National Science Foundation (*Grants Nos.* DMR - 010345 and DMR - 0422949). Partial support of U.S. Civilian Independent States of the Former Soviet Union (Contract No. UP1-2566-KH-03) is acknowledged.

APPENDIX A

The iteration method commonly used to fit theoretical and experimental curves is quite good when broadening is small. However, as the broadening Γ becomes comparable with the gap (or $\gamma > 0.3$), this introduces an appreciable uncertainty into the results. The iteration method implies that during fitting the parameters change cyclically as the step is gradually decreased. It is expected that the error reduces with each step. Our experiment shows that with high Γ (or γ) this procedure brings us finally to a local minimum point which is dependent on starting Δ , Γ (γ) and Z values and cannot correspond to the global minimum. Moreover, this method is not valid for the two-gap calculation. In our fitting procedure we therefore used the technique of coordinate descent with a postponed solution¹⁹. First, we specified an interval in which Δ is searched for at a given temperature. The interval was then subdivided into equidistant parts $\Delta_1, \Delta_2, \dots, \Delta_n$. Then Γ (γ) and Z were fitted for each Δ_i . The method used in¹⁹ does not imply that the error should decrease immediately after each Γ (or γ) step. The errors are compared after each Γ (or γ) step only when the Z -fitting is completed (this accounts for the term "postponed solution"). In the programming language, the calculation by this method reduces to embedded cycles. In the one-gap model, the Z -fitting is an inner cycle and the Γ (or γ) fitting is an outer cycle. In the two-band calculation, the Z -fitting is the innermost cycle, the fittings in Γ_1 and Γ_2 become outer and, finally, the Δ_2 -fitting is the outermost cycle. This method pro-

vides an unambiguous solution independent of the starting parameters. In the process of calculation the intensities of the theoretical and experimental curves were equalized and aligned over the ordinate before each step of calculation of the average *rms* deviation $F(\Delta_i)$. To do this, the y -coordinates of the points in the theoretical curve were multiplied by the scale factor S (the procedure of making the amplitudes of the theoretical and experimental curves equal). The curve was then shifted along the y -axis by amount B . The values of S and B were found from the condition of the minimum $F(\Delta_i)$. The standard algorithm for determination of these coefficients known as the least-square method is considered, for instance, in³⁰. As a result, for each Δ_i we could obtain Γ_i (γ_i) and Z at which the difference between the shapes of the theoretical and experimental curves characterized by the *rms* deviation $F(\Delta_i)$ was the smallest one. The kind of calculation for different temperatures is illustrated in¹⁹ (Fig. 3). In the two-gap case, the $F(\Delta_i)$ -curves are more flattened, and the curve has no minimum at a temperature lower than in the one-gap case. However, before this happens, we are able, as a rule, to find quite accurately the scale-factor S which is independent of temperature but is strongly dependent on Δ (¹⁹, Fig. 4). The value of S can vary from contact to contact but it is invariant for a particular contact. To put it more accurately, at the values of $\Gamma \sim 0$, S is practically invariable for the minima in the curves $F(\Delta)$ (see Fig. 9 in¹⁹). By choosing Δ -values which correspond to the determined magnitudes of S , we can plot quite accurately the curve $\Delta(T)$ in the high-temperature region.

-
- ¹ K. H. Muller and V. N. Narozhnyi, *Rep. Prog. Phys.* **64** pp.943-1008 (2001)
 - ² H. Kim, C. -D. Hwang, and J. Ihm, *Phys. Rev. B* **52**, 4592(1995)
 - ³ L. F. Mattheiss, *Phys. Rev. B* **49**, 13279 (1994)
 - ⁴ S. B. Dugdale, M. A. Alam, I. Wilkinson, R. J. Hughes, I. R. Fisher, P. C. Canfield, T. Jarlborg and G. Santi, *Phys. Rev. Lett.* **83** No23, p.4824 (1999)
 - ⁵ P. Dervenagas, M. Bullok, J. Zaretsky, P. Canfield, B. K. Cho, B. Harmon, A. I. Goldman, and C. Stassis, *Phys. Rev. B* **52**, 9839 (1995)
 - ⁶ C. Stassis, M. Bullok, J. Zaretsky, P. Canfield, and A. I. Goldman, *Phys. Rev. B* **55**, 8678 (1997).
 - ⁷ S. Mukhopadhyay, G. Sheeta, P. Raychaudhuri and H. Takeya, *Phys. Rev. B* **72**, 014545 (2005)
 - ⁸ Y. De Wilde, M. Iavarone, U. Welp, V. Metlushko, A. E. Koshelev, I. Aranson, G. W. Crabtree, and P. C. Canfield, *Phys. Rev. Lett.* **78**, 4273 (1997)
 - ⁹ Y. De Wilde, M. Iavarone, U. Welp, V. Metlushko, A. E. Koshelev, I. Aranson, G. W. Crabtree, P. L. Gammel, D. J. Bishop, and P. C. Canfield, *Physica C* **282-287**, 355 (1997).
 - ¹⁰ P. Martinez -Samper, J. G. Rodrigo, G. Rubio -Bollinger, H. Suderow, S. Vieira, S. Lee, and S. Tajima, *Physica C* **385**, 233 (2003).
 - ¹¹ H. Nishimori, K. Uchiyama, Sh. Kaneko, A. Tokura, H. Takeya, K. Hirata and N. Nishida, *J. of the Phys. Soc. of Japan* **73**, 3247 (2004).
 - ¹² I. K. Yanson, N. L. Bobrov, C. V. Tomy, and D. McK. Paul, *Physica C* **334**, 33 (2000)
 - ¹³ L. F. Rybalchenko, I. K. Yanson, A. G. M. Jansen, P. Mandal, P. Wyder, C. V. Tomy, and D. McK. Paul, *Physica B* **218**, 189 (1996).
 - ¹⁴ I. K. Yanson and Yu. G. Naidyuk, *Fiz. Nizk. Temp.* **30**, No4, pp.261-273 (2004); *Low Temp. Phys.* **30**, No4, 355 (2004)
 - ¹⁵ G. Goll, M. Heinecke, A. G. M. Jansen, W. Joss, L. Nguen, E. Steep, K. Winzer, P. Wyder, *Phys. Rev. B* **53**, R8871 (1996).
 - ¹⁶ L. H. Nguyen, G. Goll, E. Steep, A. G. M. Jansen, P. Wyder, O. Jepsen, M. Heinecke, and K. Winzer, *J. Low Temp. Phys.* **105**, 1653 (1996).
 - ¹⁷ S. V. Shulga, S.- L. Drechsler, G. Fuchs, K. -H. Muller, K. Winzer, M. Heinecke, and K. Krug, *Phys. Rev. Lett.* **80**, No8, 1730 (1998)
 - ¹⁸ T. Takasaki, T. Ekino, T. Muranaka, T. Ichikawa, H. Fujii, J. Akimutsu, *Phys. Soc. of Japan* **73**, pp.1902-1913 (2004)
 - ¹⁹ N. L. Bobrov, S. I. Beloborod'ko, L. V. Tyutrina, I. K. Yanson, D. G. Naugle and K. D. D. Rathnayaka, *Phys. Rev. B* **71**, 014512 (2005)

- ²⁰ A. Plecenik, M. Grajacar, S. Benacka P. Seidel, A. Pfuch, *Phys. Rev. B* **49**, 10016 (1994)
- ²¹ S. I. Beloborodko, *Fiz. Nizk. Temp.* **29**, 868 (2003): *Low Temp. Phys.* **29**, 650 (2003).
- ²² B. K. Cho, P. C. Canfield, and D. C. Johnston, *Phys. Rev. B* **52**, R3844 (1995).
- ²³ Yu. G. Naidyuk, D. L. Bashlakov, *Private communication*
- ²⁴ P. N. Chubov, A. I. Akimenko, I. K. Yanson, *A Method for Obtaining Pressed Microcontacts Between Metallic Electrodes* Author Certificate: pat. No. 83408 (USSR). Published V. I., Moscow, No20 (1981)
- ²⁵ B. N. Engel, G. G. Ihas, E. D. Adams, C. Fombarlet, *Rev. Sci. Inst.* **55**, 1489 (1984)
- ²⁶ G. E. Blonder, M. Tinkham and T. M. Klapwijk, *Phys. Rev. B* **25**, 4515 (1982)
- ²⁷ K. Maki, P. Thalmeier, and H. Won, *Phys. Rev. B* **65**, 140502(R) (2002)
- ²⁸ V. L. Pokrovsky, *Zh. Eksp. Teor. Fiz.* **40**, v.2, 641 (1961)
- ²⁹ V. L. Pokrovsky, M. S. Ryvkin, *Zh. Eksp. Teor. Fiz.* **43**, v.1, 92 (1962)
- ³⁰ D. Kahaner, C. Moler, and S. Nash, *Numerical Methods and Software* 1st ed., (Prentice-Hall, Pearson Education Company, Upper Saddle River, NJ, 1989).